Biochimica et Biophysica Acta, 1017 (1990) 125–138
Elsevier

BBABIO 43211

Soluble cytochromes and ferredoxins from the marine purple phototrophic bacterium, *Rhodopseudomonas marina*

T.E. Meyer, V. Cannac, J. Fitch, R.G. Bartsch, D. Tollin, G. Tollin and M.A. Cusanovich

Department of Biochemistry, University of Arizona, Tucson, AZ (U.S.A.)

(Received 16 November 1989)

Key words: Electron transfer protein; Cytochrome *c*; Ferredoxin; Purple bacteria; Yellow protein; (*Rps. marina*)

Four soluble *c*-type cytochromes, the high redox potential 4-Fe-S ferredoxin known as HiPIP, a large molecular weight 2-Fe-S ferredoxin and a 4-Fe-S 'bacterial' ferredoxin, were isolated from extracts of two strains of *Rps. marina*. Cytochrome *c*-550, cytochrome *c'* and cytochrome *c*-549 were previously described, and we have extended their characterization. Cytochrome *c*-558, which has not previously been observed in *Rps. marina*, appears to be a low-spin isozyme of the more commonly observed high-spin cytochrome *c'*. HiPIP, which was not observed in previous work, was found to be abundant in *Rps. marina*. The 2-Fe-S ferredoxin, which has previously been observed only in *Rps. palustris*, has a native size greater than 100 kDa and a subunit size of 17 kDa. The 'bacterial' ferredoxin appears to have only a single four-iron-sulfur cluster. We examined photosynthetic membranes by difference spectroscopy and found abundant *c*-type cytochromes. Approximately one-quarter of the heme can be reduced by ascorbate and the remainder by dithionite. There is 2 nm difference between the high-potential heme (554 nm) and the low (552 nm). These characteristics resemble those of the tetraheme reaction center cytochrome of *Rps. viridis*. In addition to the electron transfer components, we found small amounts of a fluorescent yellow protein which has spectral resemblance to a photoactive yellow protein from *Ec. halophila*.

Introduction

There are only a small number of marine bacteria presently described in the family Rhodospirillaceae. *Rb. sulfidophilus* was the first to be characterized [1] and, along with *Rb. adriaticus*, [2] shows similarity to the well-known fresh water species *Rb. sphaeroides* and *Rb. capsulatus*. *Rps. marina* was first reported by Imhoff [3] and an additional strain having somewhat different properties was labeled *Rps. marina* var. *agilis* [4]. Optimal growth of *Rps. marina* is in 1–5% NaCl and no other growth factors are required. The lipid composition is unique [3] and *Rps. marina* appears to have no close relatives.

Electron transfer proteins in *Rps. marina* were reported by Henseler et al. [5], who found three soluble cytochromes, including cytochromes *c*-552, *c*-549 and *c'*. Cytochrome *c*-552 was equated with the well-known cytochrome c_2 of various non-sulfur purple bacteria because of its size and redox potential, whereas cytochrome *c*-549 has a low redox potential similar to a protein characterized in *Rb. sphaeroides* [6,7]. We have examined *Rps. marina* in greater detail for comparison with *Rps. marina* var. *agilis* and found that, although related, there are significant differences between these two strains. We find the same three proteins reported earlier [5] in both strains and have added four new soluble electron transfer components, as well as a fluorescent yellow protein, and have characterized the membrane-bound cytochromes *c*.

Materials and Methods

Rhodopseudomonas marina type strain DSM 2698 was obtained from Dr. J. Imhoff and strain *agilis* (ATCC 35601) was supplied by Dr. H. Gest. They were grown phototropically for 3 days on a complex medium containing (per liter) 1 g yeast extract, 1 g sodium acetate, 1 g sodium malate, 1 g sodium glutamate, 20 g NaCl, 2 g KH_2PO_4, 0.5 g ammonium sulfate, 0.8 g

Abbreviations: SDS-PAGE, sodium dodecyl sulfate polyacrylamide gel electrophoresis; HiPIP, high-potential iron-sulfur protein; FMN, flavin mononucleotide; FPLC, fast protein liquid chromatography.

Correspondence: T.E. Meyer, Department of Biochemistry, University of Arizona, Tucson, AZ 85721, U.S.A.

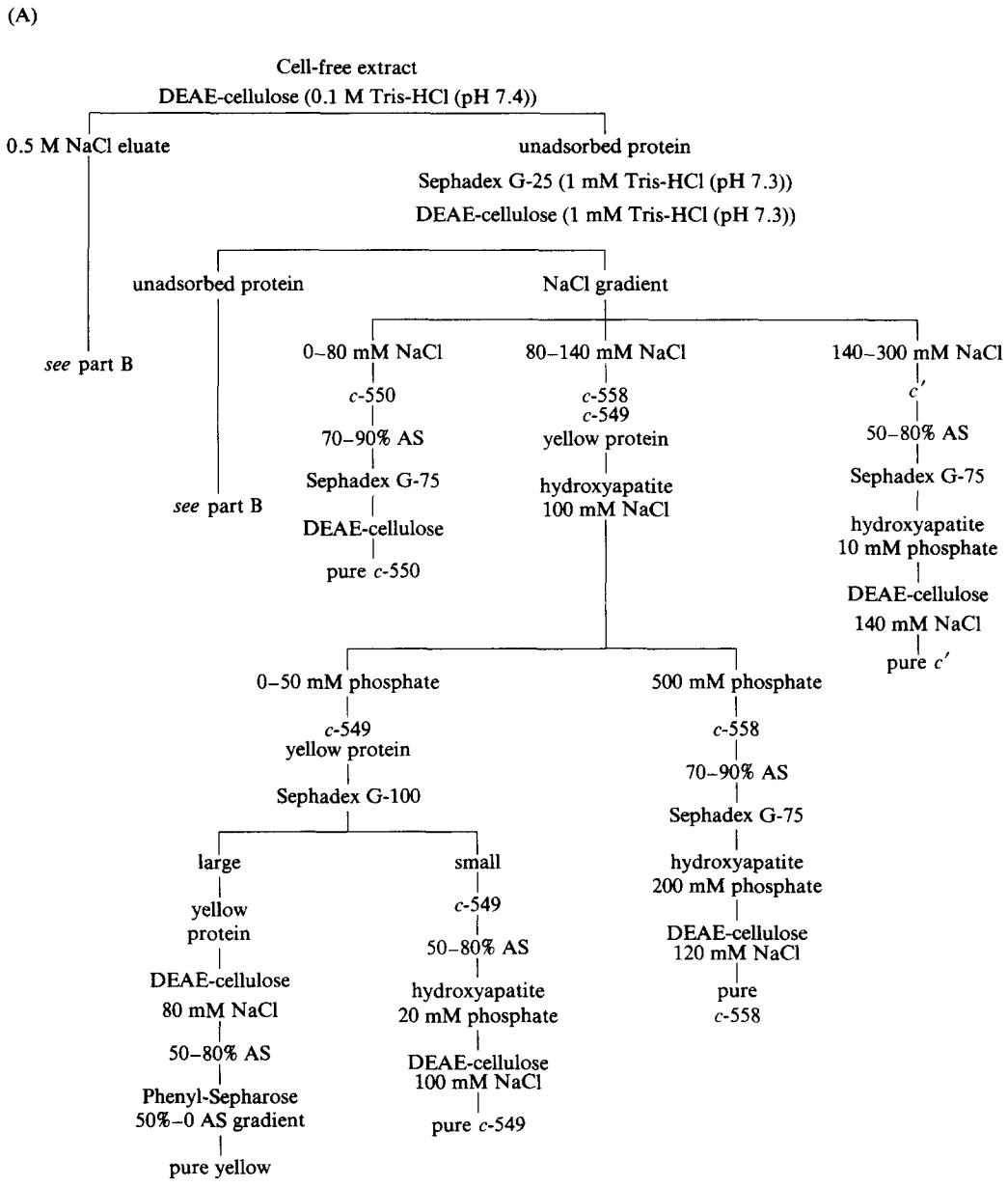

Fig. 1. Summary of protein purification. AS, ammonium sulfate; FD, ferredoxin.

$MgCl_2 \cdot 6H_2O$, 0.1 g $CaCl_2 \cdot 2H_2O$, and 1 ml Hutner's trace elements, adjusted to pH 7.

1 kg cells was suspended in 3 liters of 0.1 M Tris-HCl buffer (pH 7.5) and broken at 20 000 psi in the Ribi cell Fractionator (an automated French press). Broken cells were centrifuged 20 min in the Dupont/Sorvall SS34 rotor and for 2 h in the Beckman Spinco Type 45 Ti rotor. The Sorvall pellet was resuspended in 2 vol. of buffer and centrifuged in the Spinco. The supernatants were combined and proteins adsorbed to an 8×15 cm column of DEAE-cellulose (Whatman DE52) as described in Results.

The redox potentials of cytochrome *c*-550 and HiPIP were determined by aerobic titration of oxidized protein with ferrocyanide in 50 mM phosphate (pH 7.0). The amount of ferricyanide produced was calculated from the amount of cytochrome or HiPIP reduced. The potential of the ferri-/ferrocyanide couple was assumed to be 413 mV [8]. The redox potential of the 2-Fe-S ferredoxin was measured by anaerobic photititration of a solution containing 50 μM FMN, 10 mM EDTA and 20 mM phosphate (pH 7.0). The potential of FMN was assumed to be -206 mV [9].

The native molecular weights were measured using a Pharmacia FPLC system with a Bio-Rad TSK 125 column. An Altex Spherogel TSK SW3000 column was used for the 2-Fe-S ferredoxin only. Elution buffer contained 150 mM phosphate and 150 mM NaCl (pH 7.0). Peaks were monitored with a Hewlett-Packard Diode Array Spectrophotometer at two wavelengths,

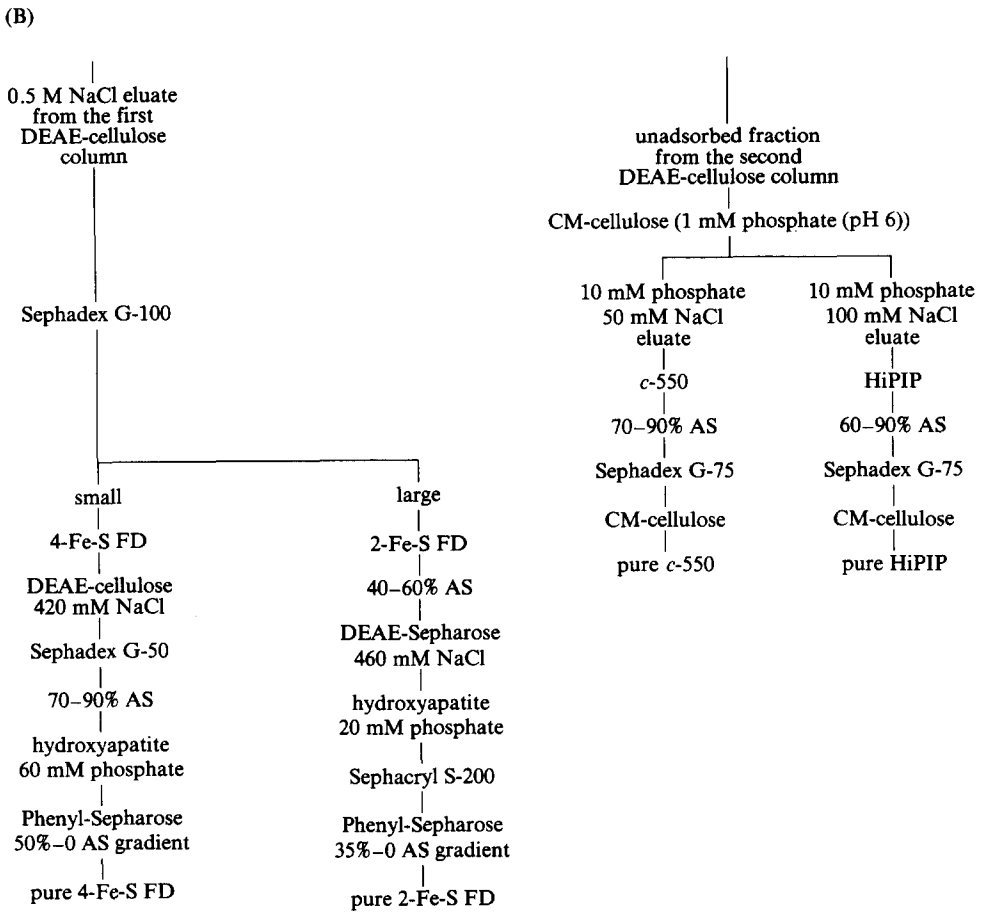

Fig. 1 (continued).

280 nm and at the visible maximum of the redox protein. Subunit sizes were measured by SDS-PAGE using the Pharmacia Phast System, with 20% cross-linked gels, stained with Coomassie blue R-250. The Bio-Rad low-molecular-weight standard kit, containing phosphorylase *b*, bovine serum albumin, ovalbumin, carbonic anhydrase, soybean trypsin inhibitor and lysozyme, was used. Isoelectric points were also measured with the Phast system using Pharmacia IEF pH 4–6.5 gels. The Pharmacia pH 3–10 broad calibration kit was used as standard. Protein was determined by the Pierce BCA protein assay method using bovine serum albumin as standard [10]. Laser flash photolysis was performed as described by Meyer et al. [11,12].

Results

A cell extract was prepared as described in Materials and Methods. All subsequent manipulations for isolation and purification of electron transfer proteins are summarized in Fig. 1. The extract was first adsorbed to an 8 × 15 cm DEAE-cellulose column. This column was washed with 20 mM Tris-HCl and eluted with 0.5 M NaCl. This fraction contained two low redox potential ferredoxins and was frozen for later purification.

DEAE-cellulose chromatography

That portion of the extract which did not adsorb to the first DEAE-cellulose column was desalted on Sephadex G-25 and adjusted to pH 7.5 in 1 mM Tris-HCl. Another 8 × 15 cm column of DEAE-cellulose adsorbed more of the proteins in the extract. This column was washed with 1 mM, then 20 mM Tris-HCl, and was then chromatographed with a stepwise gradient of 20 mM increments of NaCl up to 0.2 M and then in 0.1 M increments up to 0.5 M. In the type strain, 24 μmol cytochrome *c*-550 was eluted between 0 and 80 mM NaCl. Between 80 and 120 mM NaCl, a mixture of cytochrome *c*-558, cytochrome *c*-549 and a yellow protein was eluted. About 30 μmol total cytochrome *c′* was eluted at all salt concentrations above 140 mM and more was eluted after overnight equilibration with 0.5 M NaCl.

CM-cellulose chromatography

That portion of the bacterial extract, which did not

adsorb to DEAE-cellulose, was adjusted to pH 6 and adsorbed to a 5 × 10 cm column of CM-cellulose. HiPIP was the only colored protein to be adsorbed to CM-cellulose from an extract of the type strain. About 15 μmol was eluted with 100 mM NaCl in 10 mM phosphate.

Strain *agilis* behaved differently in that a portion of the cytochrome *c*-550 was adsorbed to both DEAE- and CM-cellulose. It was later discovered that cytochrome *c*-550 was not very soluble at low ionic strength and may have precipitated on the DEAE-cellulose column. Nevertheless, the total cytochrome *c*-550 recovered from the 80 mM NaCl wash of DEAE-cellulose and 50 mM NaCl plus 10 mM phosphate eluate of CM-cellulose was about 3 μmol. The HiPIP from strain *agilis* eluted from CM-cellulose in two bands: about 8 μmol iso-2 HiPIP at 100–120 mM NaCl and 10 μmol iso-1 HiPIP at 170–190 mM NaCl plus 10 mM phosphate (pH 7.0).

HiPIP

HiPIP fractions were purified by precipitation at 60–90% saturated ammonium sulfate, by chromatography on Sephadex G-75 and by linear gradient chromatography on CM-cellulose. Reduced HiPIP eluted ahead of the oxidized form. The best ratio of 280 nm to 400 nm absorbance was 1.40 for oxidized and 1.80 for reduced HiPIP. This is within the range expected for HiPIPs containing one tryptophan. Absorption spectra are shown in Fig. 2. The redox potential of *agilis* HiPIP is 345 mV (in 50 mM phosphate (pH 7.0)) for both isozymes. The native size is about 10 kDa and the subunit size is about 9 kDa. The first 36 residues of the N-terminal sequence of strain *agilis* iso-1 HiPIP are:

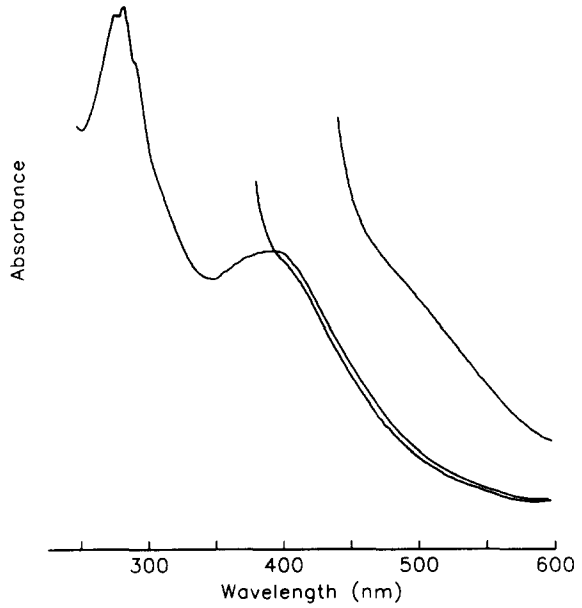

Fig. 2. Ultraviolet-visible absorption spectrum of *Rps. marina* HiPIP in 0.1 M phosphate (pH 7.0). Note the large increase in visible absorbance upon addition of ferricyanide and return upon addition of dithionite.

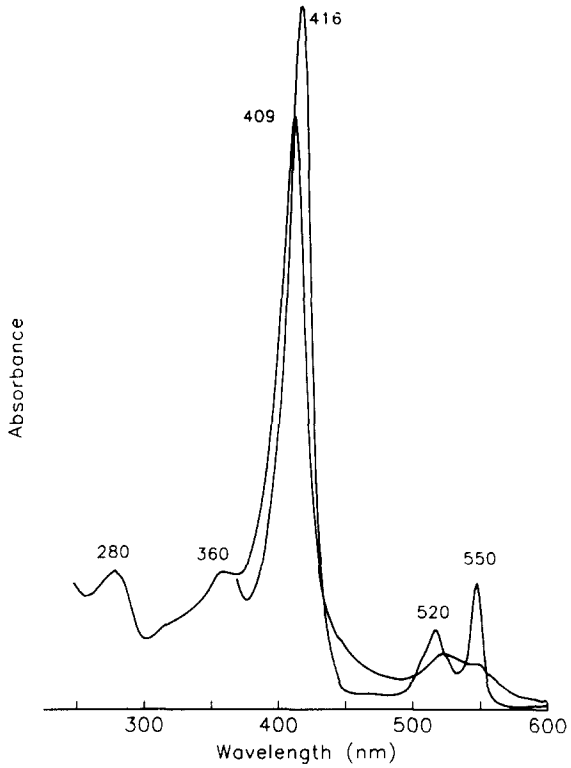

Fig. 3. Oxidized and (dithionite) reduced ultraviolet-visible absorption spectra of *Rps. marina* cytochrome *c*-550 in 0.1 M phosphate (pH 7.0).

IANKAKQAIAGYQTTPKGRQEXD

NXXXFQAADAXKV....

The unidentified residues at positions 22, 25 and 34 are probably cysteines by analogy to other HiPIP's. Iso-2 HiPIP has a blocked N-terminus.

Cytochrome c-550

The combined cytochrome *c*-550 fractions were purified by precipitation with 70–90% saturated ammonium sulfate, by Sephadex G-75 chromatography and by linear gradient chromatography on DEAE- or CM-cellulose as appropriate (type strain on DEAE- and strain *agilis* on CM-cellulose). The best ratio of 280 nm to 417 nm absorbance is 0.20. This ratio suggests the presence of two tryptophans. The absorption spectra are shown in Fig. 3. Both native and subunit sizes are about 14 kDa. The isoelectric point of strain *agilis* cytochrome *c*-550 is about 8.6 and that of the type strain about 5.0. The reduced alpha peak extinction coefficient is about 25.0 $mM^{-1} \cdot cm^{-1}$. The redox potential of the type strain cytochrome *c*-550 is 340 mV and for strain *agilis* is 320 mV (in 50 mM phosphate (pH 7.0)). Edman degradation showed that the N-terminus of both proteins was blocked. Laser flash photolysis in the presence of EDTA and FMN [11], generated flavin semiquinone which in turn reduced the cytochrome *c*-550. Second-order rate constants are plotted versus ionic strength in Fig. 4. The rate con-

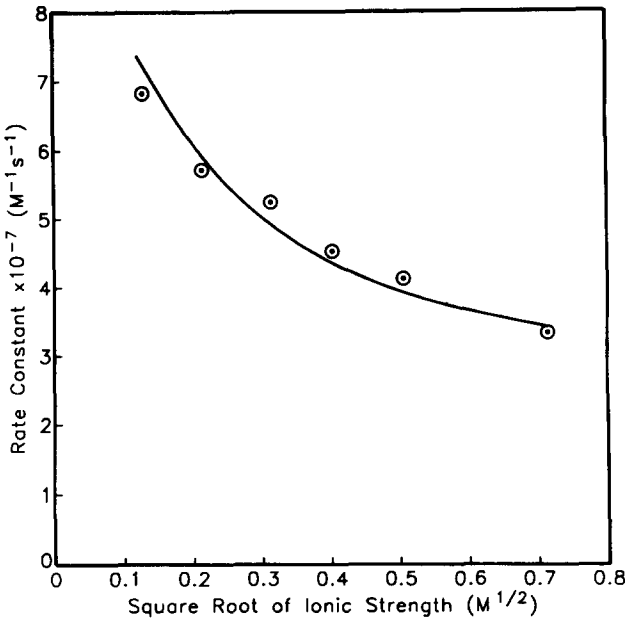

Fig. 4. Second-order rate constants versus square root of ionic strength for reduction of *Rps. marina* cytochrome *c*-550 by laser-generated FMN semiquinone. See Materials and Methods for experimental details.

stants decrease as the ionic strength is increased, indicative of a plus-minus charge interaction. Curve fitting allowed estimation of a charge of +1.8 at the site of reduction of the cytochrome from both strains.

Acidic mixture

The 80–140 mM NaCl elute of the second DEAE-cellulose column primarily contained a mixture of cytochrome *c*-558, cytochrome *c*-549 and a yellow protein with trace amounts of cytochrome *c*-550 and cytochrome *c'*. The cytochrome *c*-558 was separated by adsorption on a 2 × 4 cm column of hydroxyapatite equilibrated with 100 mM NaCl. The 50 mM phosphate eluate of the column was added to the fraction which was not adsorbed and cytochrome *c*-558 was then eluted with 0.5 M phosphate. About 5 μmol cytochrome *c*-558 was obtained from strain *agilis* and about 0.5 μmol from the type strain.

Cytochrome c-558

Strain *agilis* cytochrome *c*-558 was further purified by precipitation with 70–90% saturated ammonium sulfate, by Sephadex G-75 chromatography, by hydroxyapatite chromatography utilizing a 100–400 mM phosphate linear gradient (elution at 200 mM phosphate (pH 7)) and finally by 5–200 mM NaCl linear gradient chromatography on DEAE-cellulose (elution at 120 mM NaCl). The best ratio of 280 nm to 419 nm absorbance was 0.16. The absorption spectra are shown in Fig. 5. The extinction coefficient of the reduced alpha peak is about 21.8 $mM^{-1} \cdot cm^{-1}$. The native size is 38 kDa and the subunit is about 14 kDa. Cytochrome *c*-558 has a very weak absorbance peak at 695 nm as contrasted with cytochrome *c*-550 as shown in Fig. 6. A 695 nm peak is considered to be indicative of a methionine sixth ligand to the heme, although the absence of 695 nm absorption cannot be used to exclude methionine. We believe that methionine is the sixth ligand, in spite of the weak 695 nm absorbance.

Cytochrome c-549

Cytochrome *c*-549 and the yellow protein were resolved on Sephadex G-100 with cytochrome *c*-549 eluting after the yellow protein. About 2 μmol cytochrome *c*-549 was found in strain *agilis* and about 5 μmol in the type strain. Cytochrome *c*-549 from strain *agilis* was further purified by precipitation with 50–80% saturated ammonium sulfate. It was dissolved and adsorbed to hydroxyapatite and the column developed with a linear 0–100 mM phosphate gradient in 0.1 M NaCl (the cytochrome eluted at 20 mM phosphate). Cytochrome *c*-549 was finally chromatographed on DEAE-cellulose with a 50–150 mM NaCl linear gradient, whereupon it eluted at 100 mM NaCl. The best ratio of 280 nm to 410 nm absorbance was 0.12. The absorption spectra are shown in Fig. 7. The native size was about 12 kDa and the subunit was about 7 kDa. There were 8 mg protein per μmol heme, which indicates that there is

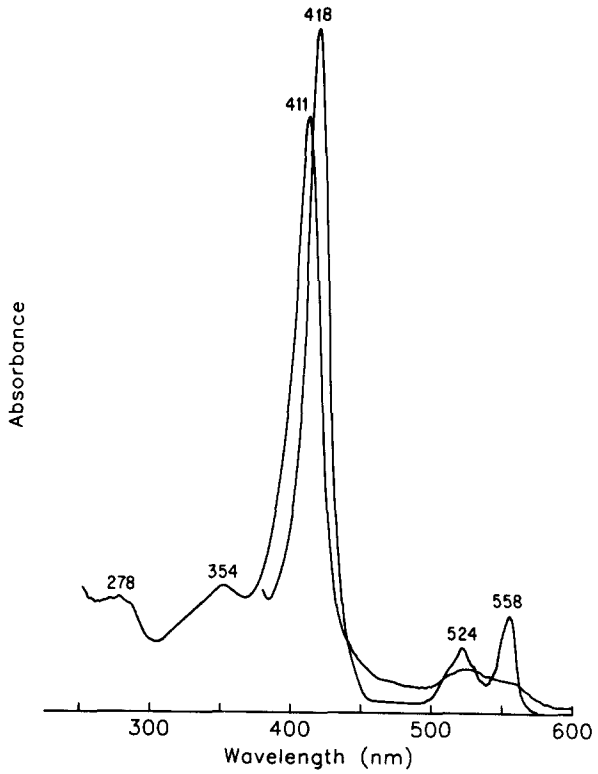

Fig. 5. Oxidized and (dithionite) reduced ultraviolet-visible absorption spectra of *Rps. marina* cytochrome *c*-558 in 0.1 M phosphate (pH 7.0). Note that all peaks are red-shifted relative to cytochrome *c*-550, except the delta peak.

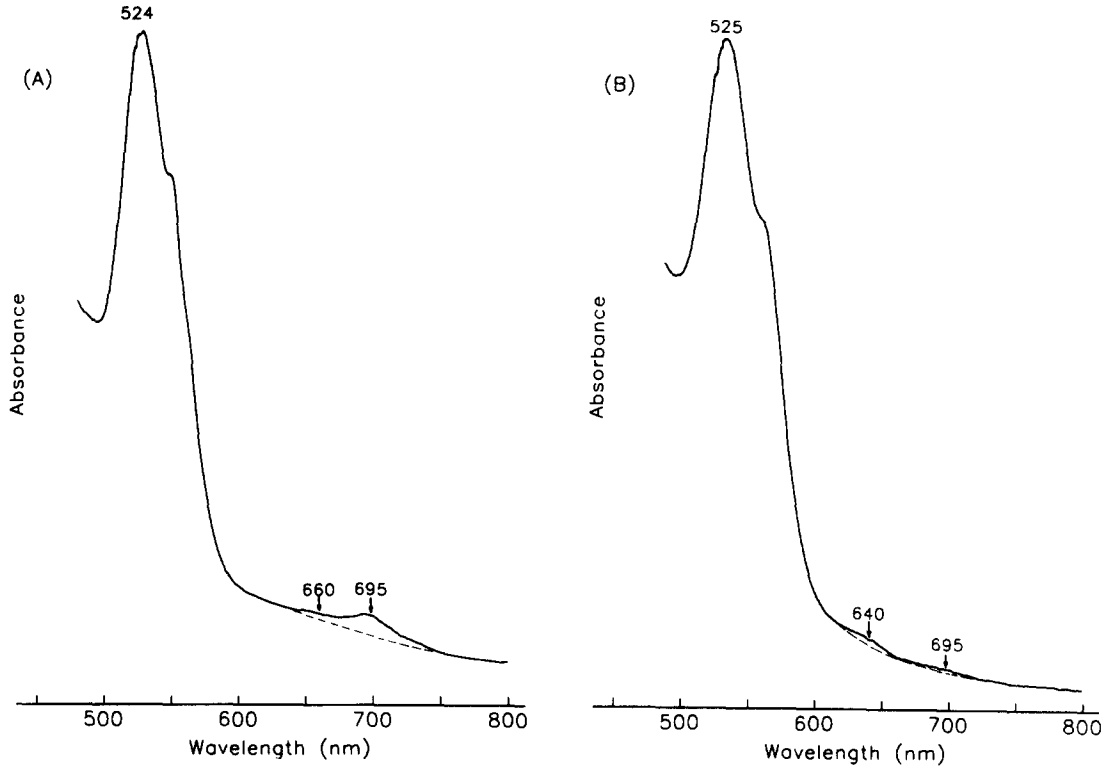

Fig. 6. Visible absorption spectra of oxidized *Rps. marina* cytochrome *c*-550 (A) and cytochrome *c*-558 (B) showing weak bands near 700 nm. Note the presence of bands near 650 nm which are indicative of some high-spin heme.

only a single heme per monomer. The redox potential is about −150 mV (in 50 mM phosphate (pH 7)) and the isoelectric point is about 4.5. The extinction coefficient of the reduced alpha peak is about 23.8 $mM^{-1} \cdot cm^{-1}$ per heme. The helix content is about 35% measured by far-ultraviolet circular dichroism spectroscopy, as shown in Fig. 8.

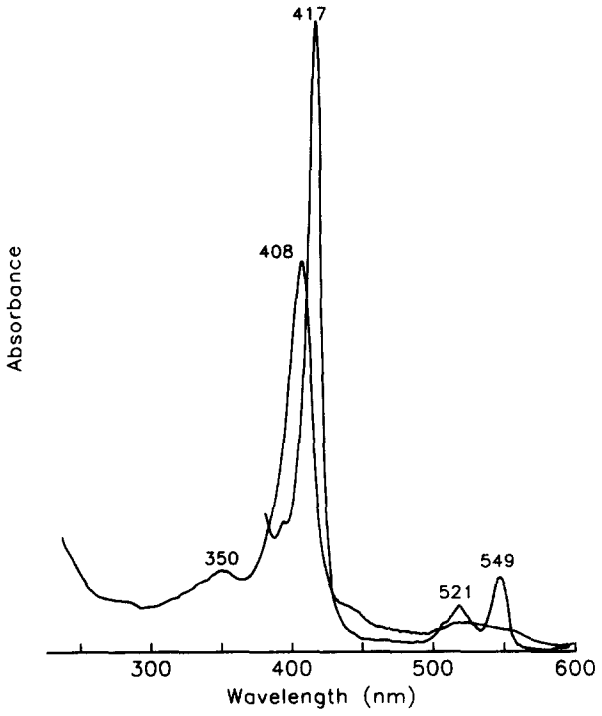

Fig. 7. Oxidized and (dithionite) reduced ultraviolet-visible absorption spectra for *Rps. marina* cytochrome *c*-549 in 0.1 M phosphate (pH 7.0). Note the near absence of 280 nm absorbance, the large increase in absorbance in the Soret on reduction and the truncated alpha peak.

Yellow protein

The type strain yellow protein which was separated from cytochrome *c*-549 on Sephadex G-100 was purified by chromatography on DEAE-cellulose using a linear gradient of 50–150 mM NaCl. About 2 μmol was eluted at 80 mM NaCl. The protein was next precipi-

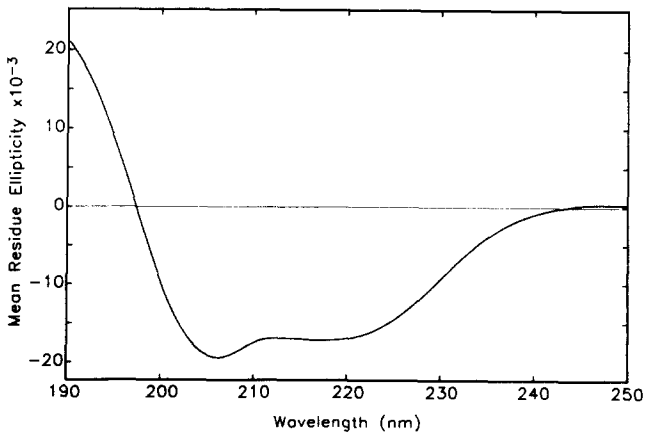

Fig. 8. Far-ultraviolet circular dichroism spectrum of *Rps. marina* cytochrome *c*-549 in water. Note the double minimum at 205 and 220 nm characteristic of alpha helix.

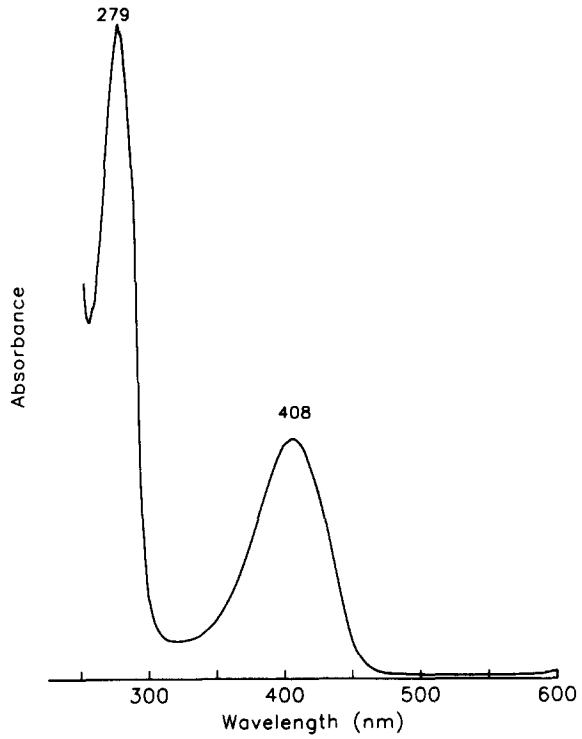

Fig. 9. Ultraviolet-visible absorption spectrum of *Rps. marina* yellow protein in 0.1 M phosphate (pH 7.0). Note the absence of absorption above 475 nm. The spectrum is unaffected by ferricyanide or dithionite.

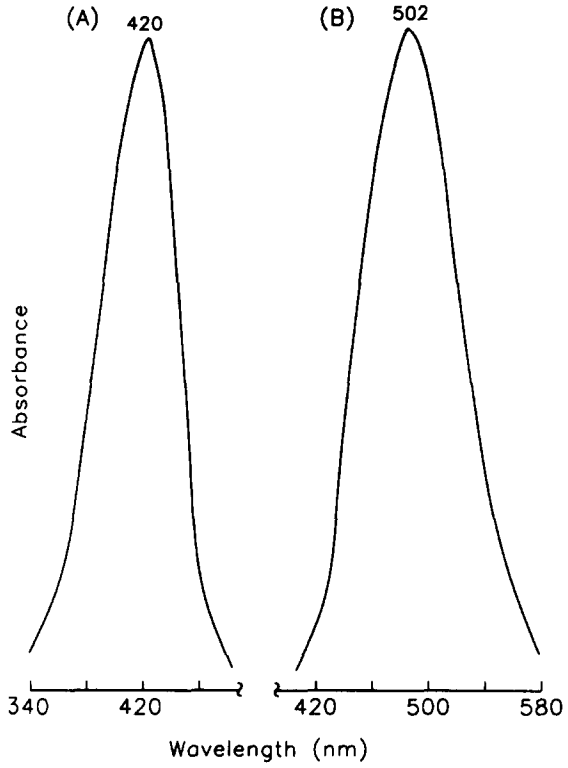

Fig. 10. Fluorescence spectrum of *Rps. marina* yellow protein in 0.1 M phosphate (pH 7.0). (A) Uncorrected excitation spectrum for emission at 502 nm; (B) uncorrected emission for excitation at 408 nm.

tated by 50–80% saturated ammonium sulfate. Final purification was by adsorption to Phenyl-Sepharose (Pharmacia) from 50% saturated ammonium sulfate, followed by a 50%–0 saturated ammonium sulfate reverse linear gradient chromatography. The protein came off the column at about 12% saturated ammonium sulfate. The best ratio of 280 nm to 408 nm absorbance was 2.6. The absorption spectrum is shown in Fig. 9. The extinction coefficient at 408 nm is 27 $mM^{-1} \cdot cm^{-1}$. The native size is about 63 kDa and the subunit is about 38 kDa. The isoelectric point of the yellow protein is 4.6. We tested the yellow protein for photoactivity because of the similarity of its absorption spectrum to a photoactive yellow protein from *Ec. halophila* [12], but found none. Instead, the yellow protein is fluorescent as shown in Fig. 10. The *Ec. halophila* yellow protein is composed entirely of beta secondary structure [13]. We therefore examined the far-ultraviolet circular dichroism spectrum as shown in Fig. 11, which indicates that the *Rps. marina* yellow protein contains 75% helical secondary structure.

Cytochrome c′

About 30 μmol of cytochrome *c′* were found in the type strain and about 5 μmol in strain *agilis*. The type strain cytochrome *c′* was precipitated by 50–80% saturated ammonium sulfate and chromatographed on Sephadex G-75, which removed residual cytochrome *c*-549. A portion of the cytochrome *c′* adsorbed to hydroxyapatite (used primarily to remove residual cytochrome *c*-558). This column was developed with a 0–50 mM phosphate gradient (the cytochrome *c′* eluted at about 10 mM phosphate without much improvement in purity). Cytochrome *c′* was finally chromatographed on DEAE-cellulose using a 50–200 mM NaCl linear gradient which eluted it at 140 mM NaCl. The best ratio of 280 nm to 400 nm absorbance was 0.23. The absorption

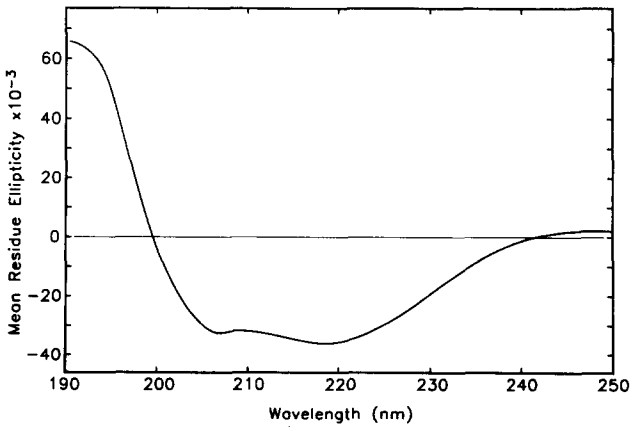

Fig. 11. Far-ultraviolet circular dichroism spectrum of *Rps. marina* yellow protein in water. Note the large ellipticity and double minimum at 205 and 220 nm indicative of alpha helix.

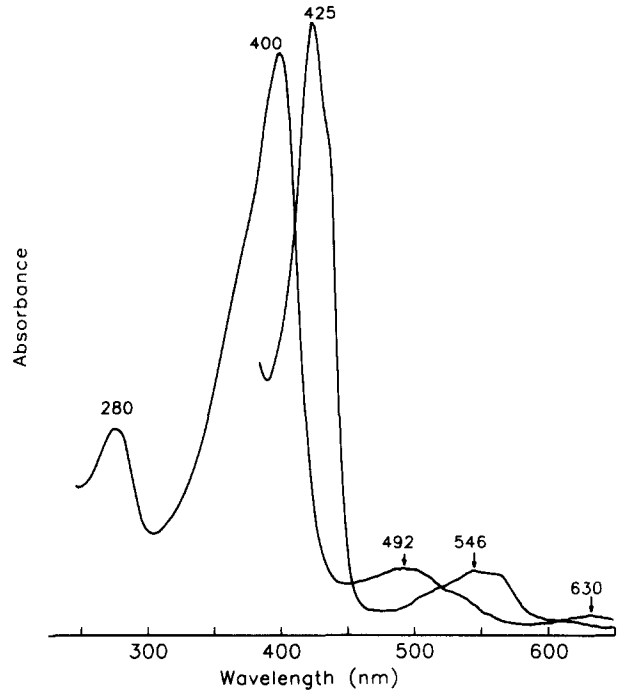

Fig. 12. Oxidized and (dithionite) reduced ultaviolet-visible absorption spectra of *Rps. marina* cytochrome *c'* in 0.1 M phosphate (pH 7.0).

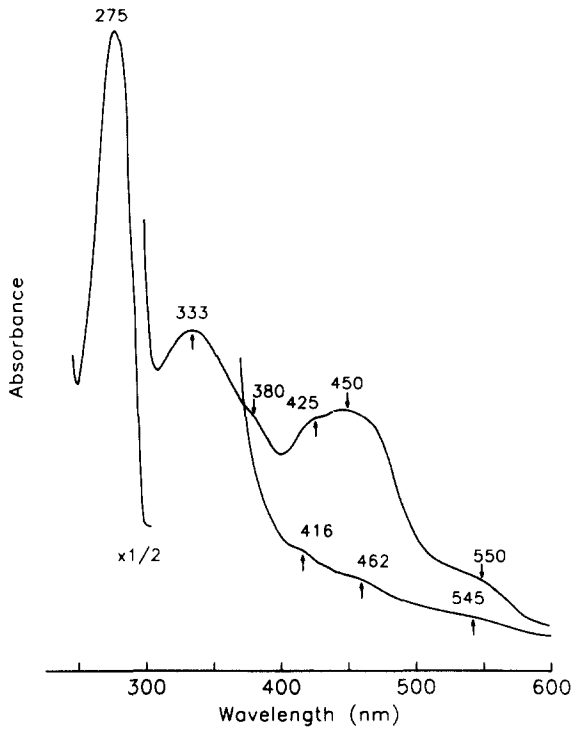

Fig. 13. Oxidized and (dithionite) reduced ultraviolet-visible absorption spectra of *Rps. marina* 2-Fe-S ferredoxin in 0.1 M phosphate (pH 7.0).

spectra are shown in Fig. 12. The native size was about 40 kDa and the subunit size was about 14 kDa.

2-Fe-S ferredoxin

The ferredoxin fraction from the first DEAE-cellulose column was chromatographed on Sephadex G-100, which separated a large 2-Fe-S ferredoxin (about 6 μmol in strain *agilis*) from a small 4-Fe-S ferredoxin (about 2 μmol). The large ferredoxin was precipitated by 40–60% saturated ammonium sulfate, dialyzed and adsorbed to a 6×15 cm column of DEAE-Sepharose (Pharmacia) in a diffuse band. Because the protein was thought to be very acidic, the column was washed with 0.2 M NaCl, which unexpectedly eluted it in a sharp band without any change in purity. It was again desalted and adsorbed to DEAE-Sepharose. This column was developed with a 40–240 mM NaCl gradient, which did not move the protein, then with a 240–720 mM NaCl gradient, which eventually eluted the ferredoxin at about 460 mM NaCl. Sephacryl S-200 chromatography was used to remove a major 50 kDa impurity. The ferredoxin was then adsorbed to hydroxyapatite (again in a diffuse band) and chromatographed with a 0–50 mM phosphate linear gradient. It eluted at about 20 mM phosphate, but trailed badly on the column. The leading fraction appeared to be nearly pure whereas the trailing fraction was still mixed with impurities. The ferredoxin was finally adsorbed to Phenyl-Sepharose from 35% saturated ammonium sulfate. The column was developed with a 35%–0 ammonium sulfate reverse linear gradient, whereupon the ferredoxin was eluted by water at the end of the gradient. The best 280 nm to 460 nm ratio was about 4.5. The absorption spectra are shown in Fig. 13. The far-ultraviolet circular dichroism spectrum is shown in Fig. 14, which indicates about 33% helical secondary structure. The ultraviolet-visible circular dichroism spectrum shown in Fig. 15 indicates some similarity to those of other 2-Fe-S ferredoxins. The native size appears to be 158 ± 10 kDa and the subunit size is about 17 kDa, with minor bands at 34 and 66 kDa, which is interpreted as incomplete dissoci-

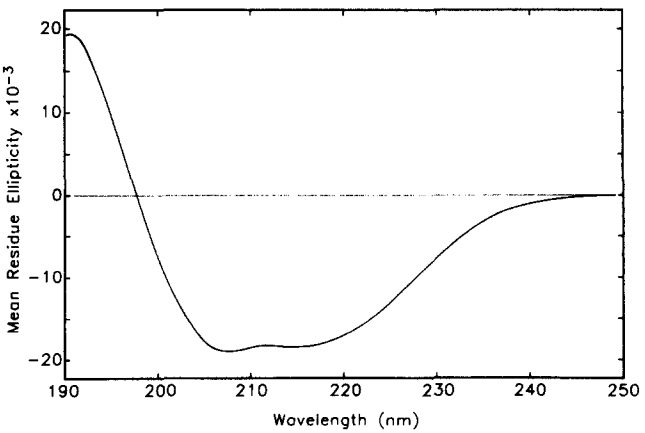

Fig. 14. Far-ultraviolet circular dichroism spectrum of *Rps. marina* 2-Fe-S ferredoxin in water.

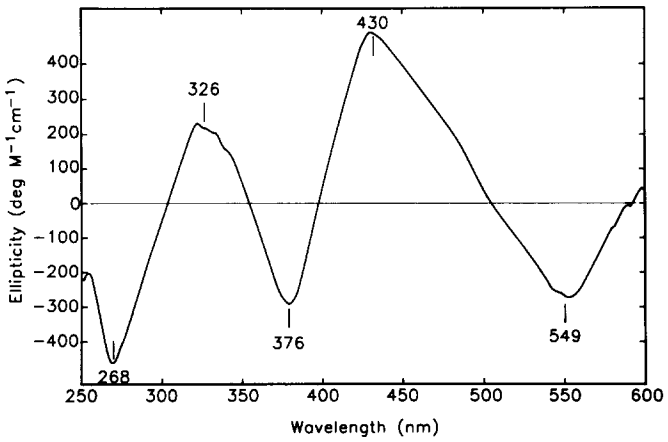

Fig. 15. Ultraviolet-visible circular dichroism spectrum of *Rps. marina* 2-Fe-S ferredoxin in water.

ation of what may be a native hexameric form. The redox potential is about −280 mV.

4-Fe-S 'bacterial' ferredoxin

The small ferredoxin from Sephadex G-100 was adsorbed to DEAE-Sepharose, chromatographed with a linear gradient of 240–480 nm NaCl plus buffer, and was eluted at about 420 mM NaCl. The ferredoxin was chromatographed on Sephadex G-50 and then precipitated by 60–90% saturated ammonium sulfate. It was next adsorbed to hydroxyapatite and chromatographed with a 0–100 mM phosphate linear gradient. It was eluted at about 60 mM phosphate. The best ratio of 280 nm to 400 nm absorbance was 2.0. The absorption spectrum is shown in Fig. 16. Both the native and subunit sizes appear to be about 18 kDa. There is about 15 mg protein per μmol 4-Fe-S cluster, which if the protein is pure indicates only a single cluster per protein.

Membrane-bound cytochromes

Photosynthetic membranes from the high-speed centrifugation of broken cells was resuspended in 0.1 M phosphate buffer (pH 7), homogenized and clarified by a short centrifugation at low speed. Difference absorption spectra were recorded on an Aminco DW2 spectrophotometer. As shown in Fig. 17, only a very small amount of cytochrome is present in the reduced form and less than one-quarter has a potential high enough to be reduced by ascorbate. The remainder is reduced by dithionite. The high-potential heme has alpha peak maximum at 554 nm and the low potential heme at 552 nm. All the cytochrome appears to be of *c*-type. The dithionite minus ascorbate spectrum (not shown) has alpha maximum at 552 nm and Soret at 423 nm. There is no long-wavelength shoulder on the 552 nm maximum which would indicate low-potential *b*-type heme such as to be expected in a cytochrome bc_1 complex. These results, along with the large cytochrome peak

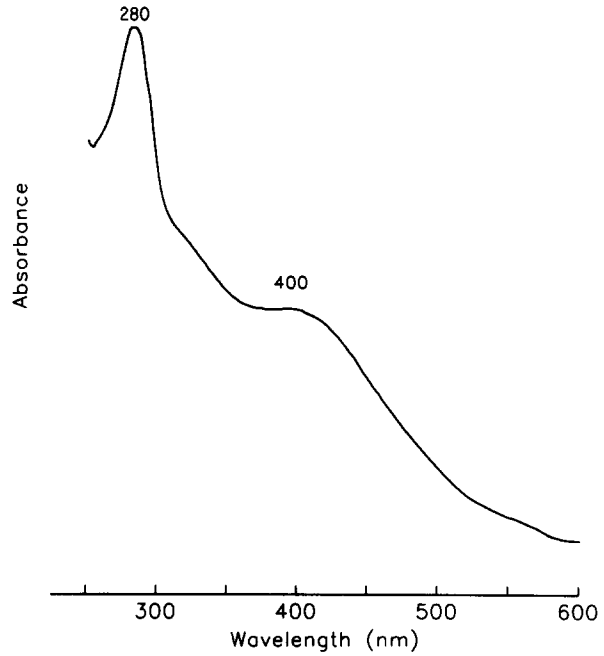

Fig. 16. Ultraviolet-visible absorption spectrum of the oxidized form of *Rps. marina* 4-Fe-S ferredoxin in 0.1 M phosphate (pH 7.0). Note the similarity of the spectrum to that of reduced HiPIP, Flg. 1. The visible absorbance bleaches slightly with either ferricyanide of dithionite.

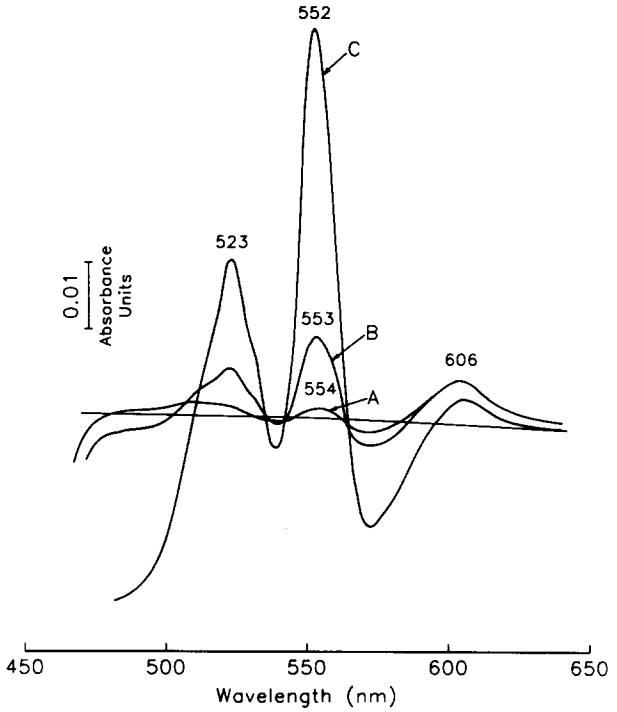

Fig. 17. *Rps. marina* photosynthetic membrane difference spectra in 0.1 M phosphate (pH 7.0). (A) As is, minus ferricyanide; (B) ascorbate minus ferricyanide; (C) dithionite minus ferricyanide. All curves were arbitrarily set to approximately zero absorbance at about 543 and 564 nm. Note that the highest redox potential cytochrome absorbs at the longest wavelength (554 nm). The 606 nm peak is due to bacteriochlorophyll. The dithionite-minus-ascorbate difference spectrum (not shown) is very similar to curve (C) and gives no indication of a low-potential *b*-type cytochrome. The dithionite-minus-ascorbate Soret is at 423 nm.

relative to that of bacteriochlorophyll, suggest the presence of a tetraheme reaction center cytochrome, which overshadows the bc_1 complex.

Discussion

We purified seven electron transfer proteins from extracts of *Rps. marina*. Three of these were previously reported by Henseler et al. [5]. The high redox potential cytochrome *c*-550 was equated with the well-known cytochrome c_2 by these workers, although other types of high-potential cytochrome have been described in purple bacteria, such as *Rc. tenuis* cytochrome *c*-553 [14]. The only certain way to identify cytochrome c_2 is though sequence determination. *Rps. marina* cytochrome *c*-550 has a blocked N-terminus, but we are now determining the complete amino-acid sequence. Another method for identifying cytochrome c_2 relies on the fact that all cytochromes c_2 have positive charge near the edge of the heme where electron transfer takes place, regardless of the overall charge on the protein. Meyer et al. [11] showed that the rate constant for reduction of cytochromes by FMN semiquinone, studied as a function of ionic strength, could be used to determine the sign and magnitude of the charge at the site of reduction. Although the type strain cytochrome *c*-550 has an isoelectric point of 5.0–5.4 and therefore has an overall negative charge [5], there is a +1.8 charge at the site of reduction, which indicates that cytochrome *c*-550 probably was correctly identified as a cytochrome c_2.

The properties of *Rps. marina* type strain cytochrome c_2 are comparable to those of Henseler et al. [5] with a few exceptions. We found approx. 10-times as much as in the earlier study (23 μmol vs. 1.9 μmol), our protein is slightly purer (280/417 nm ratio 0.20 vs. 0.22), our redox potential is a little higher (340 mV vs. 283 mV), and the alpha peak of the ultraviolet-visible absorption spectrum of our protein is at shorter wavelength (550 nm vs. 552 nm). The smaller quantity in the earlier study may be due to more aerobic growth conditions or to incomplete breakage of cells. The difference in redox potential may be due to the method of measurement or to conditions such as ionic strength. The redox potential of strain *agilis* cytochrome *c*-550 is 320 mV, which is not significantly different from the type strain. These potentials are comparable to other species of cytochrome c_2. The average of 18 cytochromes c_2 is 340 ± 48 mV.

Cytochrome c' needs little comment, as it is commonly observed as an abundant component in purple bacteria and is easily recognized by its characteristic absorption spectra. It normally occurs as a dimer and *Rps. marina* is no exception, as the 40 kDa native size is within the range observed for other dimeric cytochromes c'.

The properties of our cytochrome c' preparation from the type strain are similar to those of Henseler et al. [5] with the following exceptions. We isolated more than 15-times as much as in the earlier study (30 μmol vs. 1.8 μmol), the purity of our protein is significantly greater (280/400 nm ratio 0.23 vs. 0.65), and the minimum size of our protein appears to be somewhat smaller (14 kDa vs. 18 kDa). The low yield in the earlier study appears to be due to incomplete breakage of cells, because both cytochromes c_2 and c' were much lower than in our study and also lower than what is normally observed for other species of non-sulfur purple bacteria (about 20 μmol). The differences in minimum size may be due to use of different standards or cross-linking of the polyacrylamide. We did not measure the redox potential of our cytochrome c', but Henseler et al. [5] report 73 mV. The average for 16 cytochromes c' is 49 ± 31 mV, thus *Rps. marina* c' is slightly higher than average.

Cytochrome *c*-549 has a low redox potential and in this respect it is similar to the low redox potential cytochrome *c*-551.5 from *Rb. sphaeroides* [7]. We observe a slightly smaller native size of 12 kDa for *Rps. marina* vs. 16 kDa for *Rb. sphaeroides*. There is also one heme per 8 kDa protein, which is like the *Rb. sphaeroides* cytochrome *c*-551.5. A possible difference is that the subunit size of *Rps. marina* cytochrome *c*-549 appears to be 7 kDa. *Rb. sphaeroides* cytochrome *c*-551.5 is monomeric, but is cleaved by endogenous proteolysis with time into an 8 kDa heme-containing fragment without alteration of spectra or redox properties. We have recently sequenced the *Rb. sphaeroides* cytochrome *c*-551.5 and have found that it is unlike any other cytochrome (Van Beeumen et al., unpublished data). The sequence of the *Rps. marina* cytochrome *c*-549 will have to be determined to assess the extent of similarity to *Rb. sphaeroides* cytochrome *c*-551.5 and to determine whether it is a dimer of monoheme subunits or has been completely cleaved during purification.

The properties of the low redox potential cytochrome *c*-549 we purified from *Rps. marina* strain *agilis* are similar to those of the type strain reported by Henseler et al. [5] with the following exceptions. We found more than 10-times as much protein (5 μmol vs. 0.36 μmol), ours has significantly higher purity (280 nm/410 nm ratio 0.12 vs. 0.65), and the wavelength maxima are slightly different (549 nm vs. 550 nm). As with the cytochromes c_2 and c', the low yield of cytochrome *c*-549 was probably due to incomplete cell disruption in the earlier study. We did not completely purify the type strain cytochrome *c*-549 and did not measure its redox potential. The strain *agilis* cytochrome *c*-549 has a redox potential comparable to that reported for the type strain (−150 mV vs. −163 mV).

Cytochrome *c*-558 was not observed in the previous study, probably because it is present at very low levels in the type strain. The alpha peak is shifted further to

the red than any other soluble *c*-type cytochrome of which we are aware. The *Rps. viridis, Ch. vinosum, Th. pfennigii* and *Rc. gelatinosus* reaction center cytochromes have hemes which absorb at 556–558 nm [15–18]. Otherwise, only the low-spin isozymes of cytochromes *c′* appear to possess markedly red-shifted absorption spectra. In *Rps. palustris* this isozyme is known as cytochrome *c*-556 [19] and in *Rb. sphaeroides* it is known as cytochrome *c*-554 [7,20]. The native size of 40 kDa and subunit size of 14 kDa of *Rps. marina* cytochrome *c*-558 suggests that it is a low-spin isozyme of cytochrome *c′* similar to the *Rps. palustris* and *Rb. sphaeroides* cytochromes. The amino-acid sequences of three of these low-spin type II cytochromes are at present known from: *Rps. palustris* [21], *Agrobacterium tumefaciens* [22] and *Rb. sphaeroides* [20]. The sequence of the *Rps. marina* cytochrome *c*-558 is needed to show whether it is actually a type II cytochrome. If so, then the sixth ligand would be a methionine, although we did not see a substantial 695 nm peak, which is usually considered to be indicative of a methionine sulfur to iron charge transfer. *A. tumefaciens* cytochrome *c*-556 has a weak 695 nm band ($\epsilon = 73\ M^{-1} \cdot cm^{-1}$) [23] and both *A. tumefaciens* and *Rps. palustris* cytochromes *c*-556 have methionine ligands as shown by NMR [24]. The three-dimensional structure of *R. molischianum* cytochrome *c′* [25] suggests that methionine 16 is the sixth ligand in the low-spin type II cytochromes *c*. In *Rb. sphaeroides,* the cytochrome *c*-554 is induced by aerobic growth [20]. We have not determined whether the levels of *Rps. marina* cytochrome *c*-558 are likewise changed under aerobic growth conditions.

HiPIP was not previously observed in *Rps. marina*, although it is abundant in both strains examined. One possible reason may be the broad and featureless absorption spectrum, which might be overlooked if concentrating on cytochromes. However, HiPIP was the only colored protein which was adsorbed to CM-cellulose in the type strain and it is easily recognized by the increase in visible absorbance on addition of ferricyanide (the iron-sulfur clusters of bacterial ferredoxin are slowly destroyed by ferricyanide, as indicated by a progressive bleach of absorbance). HiPIP is observed less frequently than either cytochrome c_2 or *c′* in non-sulfur purple bacteria, but has previously been reported in *Rc. gelatinosus* [26,27], *Rc. tenuis* [28,29], *Rm. vannielii* [28], *Rp. globiformis* (Meyer, unpublished data) and *R. salinarum* [30]. Only *Rm. vannielii* and *Rp. globiformis* are known to contain cytochrome c_2 in addition to HiPIP and this now appears to be the case in *Rps. marina.* The sequences of *Rc. gelatinosus* and *Rc. tenuis* HiPIP's are known [27,29]. Based on the N-terminal amino-acid sequence, *Rps. marina* HiPIP is most similar to that of *Rc. tenuis* (9 out of 31 identities). The function of HiPIP is unknown, but it is conceivable that it could substitute for cytochrome c_2 in some situations by virtue of its high redox potential. It was shown that HiPIP was an effective electron donor to reaction center in *Ch. vinosum* [31]. On the other hand, HiPIP does not show conservation of positive charge at the site of reduction [32] the way cytochrome c_2 does, which may render it less effective as an alternative electron donor to the reaction center or to the reaction center cytochrome in some species. *Rps. marina* HiPIP is now being tested as an electron donor to reaction center.

The 2-Fe-S ferredoxin observed in *Rps. marina* could easily have been overlooked, even though it is abundant. It adsorbs diffusely to DEAE-cellulose and its yellow-brown color is similar to that of many other soluble constituents. A two-iron-sulfur ferredoxin was previously observed in purple bacteria only in *Rps. palustris* [33]. However, two-iron-sulfur ferredoxins are commonly found in plants, algae and cyanobacteria, where they function as electron acceptors for Photosystem I. Unlike plant ferredoxin, which is a 10 kDa monomer, the two purple bacterial 2-Fe-S ferredoxins have a large native molecular weight. Purple bacteria do not have Photosystem I and presumably are unable to photoreduce low-potential electron acceptors (the normal electron acceptors are quinones, which have potentials of 0 to −100 mV). Thus, it appears that the *Rps. palustris* and *Rps. marina* ferredoxins must have some other function. 2-Fe-S ferredoxins have been reported in non-photosynthetic bacteria, but they generally have relatively low molecular weights, like plant ferredoxin. The *Halobacterium* ferredoxin has a sequence related to plant ferredoxin [34], but the *Clostridium* 2-Fe-S ferredoxin shows no obvious similarity to either [35]. It appears therefore that there are at least two types of unrelated soluble 2-Fe-S ferredoxin in bacteria, and if the membrane-bound Rieske iron-sulfur protein of the bc_1 complex is included, there are at least three types of unrelated peptide chain. The Rieske 2-Fe-S protein subunit of the cytochrome bc_1 complex is normally membrane-bound, but it is conceivable that it could be partially soluble in *Rps. marina*. However, the low redox potential of *Rps. marina* ferredoxin argues against its being a water-soluble form of the Rieske 2-Fe-S ferredoxin unless it is denatured, because the Rieske ferredoxin has a redox potential of about +200 mV.

The ultraviolet-visible absorption spectrum of the *Rps. marina* 2-Fe-S ferredoxin is more like those of the *Clostridium* ferredoxin and the Rieske iron-sulfur protein and less like those of spinach, adrenal, *E. coli* and *H. halobium* ferredoxins, particularly in the ratio of the peaks near 420 and 460 nm and in the presence of a distinct shoulder near 550 nm. The ultraviolet-visible circular dichroism spectrum of the *Rps. marina* 2-Fe-S ferredoxin is also similar to that of other ferredoxins, but is not identical to any. *E. coli, H. halobium,* spinach and adrenal ferredoxins all have CD maxima at 420 to

435 nm and 320–363 nm and minima at 550 nm, 500 nm and 360 to 390 nm [36–38]. *Rps. marina* ferredoxin has the 430 nm and 326 nm maxima and the 549 nm and 376 nm minima, but does not have a minimum at 500 nm. The *Clostridium* ferredoxin does not have the approx. 350 nm maximum nor the 500 nm minimum and has extra maxima at 400 and 465 nm [39]. The Rieske iron sulfur protein has additional maxima at 400–500 nm and does not have a minimum at 500 nm [40]. It is apparent from the spectral analyses that the *Rps. marina* protein is not identical to any of the three known types of unrelated bacterial 2-Fe-S ferredoxin (*H. halobium*, *Clostridium* and Rieske), but in fact may represent a new family. The amino-acid sequence should be determined to address this point.

'Bacterial' ferredoxins generally contain two 4-Fe-S clusters in a small protein of 6–14 kDa. The 8-Fe-S ferredoxins from the phototrophic bacteria *Chl. limicola Ch. vinosum* [41], and *Rb. capsulatus* [42] appear to be typical. Ferredoxins containing a single 4-Fe-S cluster appear to be less common, although they have been observed in the phototrophic bacteria *R. rubrum* [43] and *Rb. capsulatus* [44] in addition to the 8-Fe-S ferredoxin. The molecular weight of the phototrophic single-cluster ferredoxins is larger than the two-cluster ferredoxins (15–18 kDa), but no sequences are yet available for comparison. The single-cluster ferredoxin is constitutive in *R. rubrum* and *Rb. capsulatus*, but the two-cluster ferredoxins are induced by photosynthetic or nitrogen fixing conditions [43,44]. The *Rps. marina* ferredoxin we purified has a single cluster and a molecular weight of 18 000. It thus appears to be related to the single cluster ferredoxins from *R. rubrum* and *Rb. capsulatus*.

We previously purified an abundant, small soluble yellow protein from *Ec. halophila* [45] and subsequently found that it had photoactivity similar to sensory rhodopsin in *Halobacterium* [12]. The as yet unidentified chromophore of the *Ec. halophila* yellow protein absorbs light at 446 nm in the holo-protein and is unaffected by oxidizing or reducing agents. In *Rps. marina* (and several other species, unpublished) there is a yellow protein which has a similar chromophore but has a larger molecular weight. As is the case with the ferredoxins, there are a number of nondescript yellow proteins in the soluble fraction of bacteria, which make it difficult to identify any single protein in the mixture by spectroscopy alone. Nevertheless, we have purified a yellow protein from *Rps. marina* and have shown that it is probably unrelated to that from *Ec. halophila* (except in having an apparently similar chromophore). The *Ec. halophila* protein is photoactive, but we could not observe any photoactivity in the purified *Rps. marina* yellow protein. This is not surprising, because we found that the *Rps. marina* protein is highly fluorescent (emission maximum 502 nm). Other differences are that *Rps. marina* yellow protein is a dimer of 38 kDa subunits, whereas *Ec. halophila* yellow protein is a 14 kDa monomer. The *Ec. halophila* yellow protein three-dimensional structure shows that it is composed entirely of beta secondary structure and has no helix whatsoever [13]. On the other hand, the *Rps. marina* protein is all helical. The *Rps. marina* yellow protein has maximal absorbance at 408 nm, whereas the *Ec. halophila* yellow protein absorbs at 446 nm. Our present working hypothesis is that the *Ec. halophila* yellow protein is a photoreceptor for the negative phototactic response away from blue light in phototrophic bacteria. Although the *Rps. marina* yellow protein may have a similar chromophore, its properties are such that it almost certainly has some other function.

It appears that *Rps. marina* contains a membrane-bound tetraheme reaction center cytochrome based on the following characteristics. The cytochrome is abundant and overshadows the cytochrome bc_1. There is both high- and low-potential heme, and the high-potential heme absorbs light at longer wavelength than the low-potential heme. *Rps. marina* has one heme which absorbs at 554 nm and the remainder which absorb near 552 nm. These characteristics are more similar to those of *Chloroflexus* reaction center cytochrome, which has only a single maximum at 554 nm [46], than they are to *Rps. viridis* cytochrome, which absorbs at 558, 556 and 552 nm [47]. The *Rps. marina* cytochrome is almost completely oxidized as isolated, which suggests that the highest-potential heme has a redox potential of 250 mV or less. Only one-quarter of the heme is reduced by ascorbate, which further suggests that the remaining hemes have redox potentials less than 0–100 mV. This characteristic is also more like *Chloroflexus* reaction center cytochrome ($E_{m,7} = 300$, 220, 120, and 0 mV) [46] and less like *Rps. viridis* ($E_{m,7} = 370$, 300, 10, and -60 mV) [47].

Membrane-bound reaction center cytochromes have now been found in several species of non-sulfur purple bacteria, including, *Rps. viridis* [15,48], *Rc. gelatinosus* [18], *R. salexigens* [49] and *Rps. marina*. In contrast, *Rb. sphaeroides* [50], *Rb. capsulatus* and *R. rubrum* lack membrane-bound reaction center cytochromes. It appears that there are least as many species which have it as those which do not. All of the purple sulfur bacteria which have been examined do have the reaction center cytochrome. Thus, a majority of purple bacteria (8 of 11 species) have the cytochrome, although there is no clear explanation as to why it is conserved, since cytochrome c_2 appears to be as efficient an electron donor to reaction center as the bound cytochrome.

Marine phototrophic bacteria have not received the same attention as fresh-water bacteria and it is not known whether they are more closely related to the fresh-water or to the more halophilic bacteria. Three halophiles have been examined: *Ec. halophila* [45], *R.*

salinarum [30] and *R. salexigens* [49]. They are not very closely related to one another; *Ec. halophila* is closer to other purple sulfur bacteria, *R. salinarum* may be intermediate between sulfur and non-sulfur purple bacteria, and *R. salexigens* has a cytochrome pattern similar to fresh-water non-sulfur purple bacteria. *Rps. marina* also appears to be related to the fresh-water purple bacteria in electron transfer proteins, but amino-acid sequences are needed to establish a quantitative relationship among species.

In conclusion, we have purified seven electron transfer proteins and a fluorescent yellow protein to homogeneity from the soluble fraction of *Rps. marina*. All but the fluorescent yellow protein appear to be similar to proteins described in other species. What is unique about *Rps. marina* is the large number of such proteins. In this respect it is like *Rb. sphaeroides,* where at least seven soluble cytochromes have been purified and characterized [7,20,51]. With the exception of cytochromes c_2 and c' and HiPIP, which are commonly observed in purple bacteria, cytochromes *c*-549 and *c*-558 and the 2-Fe-S and 4-Fe-S ferredoxins are less often seen. Their characterization will greatly aid in defining new classes of electron transfer proteins and in finding roles for them. The fluorescent yellow protein has not been described previously, but appears to occur in several other species. Its characterization will open the way toward defining its distribution, structure and function in purple bacteria.

Acknowledgement

This work was supported by a grant from the NIH (DK 15057) to G.T. and from the NSF (DMB 8718678) to T.E.M.

References

1 Hansen, T.A. and Veldkamp, H. (1973) Arch. Microbiol. 92, 45–58.
2 Neutzling, O., Imhoff, J.F. and Truper, H.G. (1984) Arch. Microbiol. 137, 256–261.
3 Imhoff, J.F. (1983) System. Appl. Microbiol. 4, 512–521.
4 Mangels, L.A., Favinger, J.L., Madigan, M.T. and Gest, H. (1986) FEMS Microbiol. Lett. 36, 99–104.
5 Henseler, A., Truper, H.G. and Fischer, U. (1986) FEMS Microbiol. Lett. 33, 1–8.
6 Meyer, T.E., Bartsch, R.G. and Kamen, M.D. (1971) Biochim. Biophys. Acta 245, 453–464.
7 Meyer, T.E. and Cusanovich, M.A. (1985) Biochim. Biophys. Acta 807, 308–319.
8 O'Reilly, J.E. (1973) Biochim. Biophys. Acta 292, 509–515.
9 Draper, R.D. and Ingraham, L.L. (1968) Arch. Biochem. Biophys. 125, 802–808.
10 Smith, D.P.K., Krohn, R.I., Hermanson, G.T., Mallia, A.K., Gartner, F.H., Provenzano, M.D., Fujimoto, E.K., Goeke, N.M., Olson, B.J. and Klenk, D.C. (I1985) Anal. Biochem. 150, 76–85.
11 Meyer, T.E., Watkins, J.A., Przysiecki, C.T., Tollin, G. and Cusanovich, M.A. (1984) Biochemistry 23, 4761–4767.
12 Meyer, T.E., Yakali, E., Cusanovich, M.A. and Tollin, G. (1987) Biochemistry 26, 418–423.
13 McRee, D.E., Tainer, J.A., Meyer, T.E., Van Beeumen, J., Cusanovich, M.A. and Getzoff, E.D. (1989) Proc. Natl. Acad. Sci. USA 86, 6533–6537.
14 Ambler, R.P., Meyer, T.E. and Kamen, M.D. (1979) Nature 278, 661–662.
15 Trosper, T.L., Benson, D.L. and Thornber, J.P. (1977) Biochim. Biophys. Acta 460, 318–330.
16 Kennel, S.J. and Kamen, M.D. (1971) Biochim. Biophys. Acta 253, 153–166.
17 Seftor, R.E.B. and Thornber, J.P. (1984) Biochim. Biophys. Acta 764, 148–159.
18 Fukushima, A., Matsuura, K., Shimada, K. and Satoh, T. (1988) Biochim. Biophys. Acta 933, 399–405.
19 Bartsch, R.G. (1978) in The Photosynthetic Bacteria (Clayton, R.K. and Sistrom, W.R., eds.), pp. 249–279, Plenum Press, New York.
20 Bartsch, R.G., Ambler, R.P., Meyer, T.E. and Cusanovich, M.A. (1989) Arch. Biochem. Biophys. 271, 433–440.
21 Ambler, R.P., Bartsch, R.G., Daniel, M., Kamen, M.D., McLellan, L., Meyer, T.E. and Van Beeumen, J. (1981) Proc. Natl. Acad. Sci. USA 78, 6854–6857.
22 Van Beeumen, J., Tempst, P., Stevens, P., Bral, D., Van Damme, J. and DeLey, J. (1980) in Protides of Biological Fluids (Peeters, H., ed.), pp. 69–74, Pergamon Press, New York.
23 Van den Branden, C., Van Beeumen, J. and DeLey, J. (1975) Hoppe-Seyler's Z. Physiol. Chem. 356, 1251–1258.
24 Moore, G.R., McClune, G.J., Clayden, N.J., Williams, R.J.P., Alsaadi, B.M., Angstrom, J., Ambler, R.P. Van Beeumen, J., Tempst, P., Bartsch, R.G., Meyer, T.E. and Kamen, M.D. (1982) Eur. J. Biochem. 123, 73–80.
25 Finzel, B.C., Weber, P.C., Hardman, K.D. and Salemme, F.R. (1985) J. Mol. Biol. 186, 627–643.
26 DeKlerk, H. and Kamen, M.D. (1966) Biochim. Biophys. Acta 112, 175–178.
27 Tedro, S.M., Meyer, T.E. and Kamen, M.D. (1976) J. Biol. Chem. 251, 129–136.
28 Bartsch, R.G. (1978) Methods Enzymol. 53D, 329–340.
29 Tedro, S.M., Meyer, T.E. and Kamen, M.D. (1979) J. Biol. Chem. 254, 1495–1500.
30 Meyer, T.E., Fitch, J.C., Bartsch, R.G., Tollin, D. and Cusanovich, M.A. (1990) Biochim. Biophys. Acta 1017, 118–124.
31 Kennel, S.J., Bartsch, R.G. and Kamen, M.D. (1972) Biophys. J. 12, 882–896.
32 Przysiecki, C.T., Cheddar, G., Meyer, T.E., Tollin, G. and Cusanovich, M.A. (1985) Biochemistry 24, 5647–5652.
33 Yamanaka, T. and Kamen, M.D. (1967) Biochim. Biophys. Acta 131, 317–329.
34 Hase, T., Wakabayashi, S., Matsubara, H., Kerscher, L., Oesterhelt, D., Rao, K.K. and Hall, D.O. (1977) FEBS Lett. 77, 308–310.
35 Meyer, J., Bruschi, M.H., Bonicel, J.J. and Bovier-Lapierre, G.E. (1986) Biochemistry 25, 6054–6061.
36 Knoell, H.E. and Knappe, J. (1974) Eur. J. Biochem. 50, 245–252.
37 Kerscher, L., Oesterhelt, D., Cammack, R. and Hall, D.O. (1976) Eur. J. Biochem. 71, 101–107.
38 Palmer, G., Brintzinger, H. and Estabrook, R.W. (1967) Biochemistry 6, 1658–1664.
39 Cardenas, J., Mortenson, L.E. and Yoch, D.C. (1976) Biochim. Biophys. Acta 434, 244–257.
40 Fee, J.A., Findling, K.L., Yoshida, T., Hille, R., Tarr, G.E., Hearshen, D.O., Dunham, W.R., Day, E.P., Kent, T.A. and Munck, E. (1984) J. Biol. Chem. 259, 124–133.
41 Matsubara, H., Hase, T., Wakabayashi, S. and Wada, K. (1980) in The Evolution of Protein Structure and Function (Sigman, D.S. and Brazier, M.A.B., eds.), pp. 245–266, Academic Press, New York.

42 Hallenbeck, P.C., Jouanneau, Y. and Vignais, P.M. (1982) Biochim. Biophys. Acta 681, 168–176.
43 Yoch, D.C., Arnon, D.I. and Sweeney, W.V. (1975) J. Biol. Chem. 250, 8330–8336.
44 Yakunin, A.F. and Gogotov, I.N. (1983) Biochim. Biophys. Acta 725, 298–308.
45 Meyer, T.E. (1985) Biochim. Biophys. Acta 806, 175–183.
46 Freeman, J.C. and Blankenship, R.E. (1990) Photosynth. Res. 23, 29–38.
47 Fritszch, G., Buchanan, S. and Michel, H. (1989) Biochim. Biophys. Acta 977, 157–162.
48 Deisenhofer, J., Epp, O., Miki, K., Huber, R. and Michel, H. (1985) Nature 318, 618–624.
49 Meyer, T.E., Fitch, J.C., Bartsch, R.G., Tollin, G. and Cusanovich, M.A. (1990) Biochim. Biophys. Acta 1016, 364–370.
50 Allen, J.P., Feher, G., Yeates, T.O., Komiya, H. and Rees, D.C. (1987) Proc. Natl. Acad. Sci. USA 84, 6162–6166.
51 Fitch, J., Cannac, V., Meyer, T.E., Cusanovich, M.A., Tollin, G., Van Beeumen, J., Rott, M.A. and Donohue, T.J. (1989) Arch. Biochem. Biophys. 271, 502–507.